The Mesoscale Structure of a Nocturnal Dryline and of a Frontal–Dryline Merger

DAVID B. PARSONS

Atmospheric Technology Division, National Center for Atmospheric Research, Boulder, Colorado*

MELVYN A. SHAPIRO

National Oceanic and Atmospheric Administration/Environmental Research Laboratories/ Environmental Technology Laboratory, Boulder, Colorado

ERIK MILLER

Atmospheric Technology Division, National Center for Atmospheric Research, Boulder, Colorado*

(Manuscript received 3 March 2000, in final form 28 April 2000)

ABSTRACT

A horizontal gradient in moisture, termed the dryline, is often detected at the surface over the southern Great Plains of the United States during the spring and early summer. The dryline exhibits distinct diurnal variations in both its movement and structure. Recent research has focused on dryline structure during the afternoon and evening, particularly showing how strong ($\sim$1–5 m s^{-1}) ascent frequently creates an environment favorable to the initiation of convection, quite close (within $\sim$10 km) to the dryline interface. To date, however, there have been very few detailed analyses of the dryline interface at night, so that the nocturnal behavior of the interface predicted by theory and numerical studies is relatively poorly evaluated. In this study, special observations taken by a Doppler lidar, serial rawinsonde ascents, and a dual-channel microwave radiometer are utilized to describe the behavior of a nocturnal dryline observed on 12–13 May 1985. The analysis presented here reveals that the mesoscale structure of the nocturnal dryline prior to the formation of deep convection is a gently sloping, slow-moving interface. The movement of the dryline at night was related to the evolution of the low-level jet within the moist air. Wavelike structures and evidence for vertical mixing were observed in the moist air as low Richardson numbers occurred below the height of the jet. The previously discussed strong ascent is largely lacking in the present nocturnal case so that the circulations inherent to an undisturbed dryline at night are far less favorable for the initiation of deep convection than in the afternoon and early evening.

In the present case, severe convection developed as a weak cold front approached and merged with the nocturnal dryline and the environment rapidly destabilized. Between soundings taken 2.5 h apart, the convective available potential energy increased from 524 to 3417 J kg^{-1} and the absolute value of the convective inhibition decreased from 412 to 9 J kg^{-1}. The vertical shear of the horizontal wind also dramatically increased with time, so that the bulk Richardson number was within values normally associated with supercell convection. The timescale of the changes in stability and in the moisture field ($\sim$1–2.5 h) has implications for the type of observing network needed to nowcast severe convection and for assessing the performance of research and operational numerical models.

1. Introduction

During spring and early summer, a meoscale gradient in dewpoint temperature, termed the dryline, often develops at the surface over the southern Great Plains of the United States (e.g., Schaefer 1986). The dewpoint temperature across this boundary can vary up to $\sim$18 K in a distance of only 1 to 10 km (e.g., NSSP Staff 1963). The boundary develops as moist air from over the Gulf of Mexico flows northward over the central United States and converges with air that has passed over the dry inland plateaus and subsided in the lee of the Rocky Mountains. Rhea (1966) found that the isolated and mesoscale convective events that take place over broad expanses of this region are typically first initiated quite close (within 10 km) to the dryline. In addition, severe convection over this region is often first initiated at the dryline (McCarthy and Koch 1982; Bluestein and Parker 1993). The local nature of the convective initiation and the tendency for a sharp gradients

* The National Center for Atmospheric Research is sponsored by the National Science Foundation.

Corresponding author address: Dr. David B. Parsons, Atmospheric Technology Division, NCAR, P.O. Box 3000, Boulder, CO 80307-3000. E-mail: parsons@ucar.edu

across the interface to sometimes be present have led researchers to increasingly rely on special field campaigns and high-resolution numerical studies to better describe and diagnose the dynamics of the dryline.

It has long been noted that the dryline exhibits strong diurnal variations in response to boundary layer processes. For example, McCarthy and Koch (1982) noted a clear steepening of the dryline interface toward the vertical during the afternoon. Also, Ogura and Chen (1977) and Sun and Ogura (1979) presented evidence that the dryline could be thought of as an inland sea breeze resulting from differential surface solar heating with stronger heating over the drier, elevated terrain to the west. Under this hypothesis, a horizontal pressure gradient will result from this differential heating, creating easterly, upslope flow and a broad (~100 km) region of ascent as the surface heating progresses. Field studies of the character of the dryline during the afternoon and early evening have been generally supportive of the role of differential surface heating in dryline dynamics. For example, Parsons et al. (1991), Ziegler and Hane (1993), and Atkins et al. (1998) observed mesoscale gradients in virtual temperature within the moist air. Bluestein and Crawford (1997) further documented that an upslope component of the pressure gradient develops during the day within the moist air, followed later in the day by a corresponding increase in the upslope winds. Numerical studies have shown that differential surface heating caused by horizontal gradients in soil moisture and vegetation aids in the formation of the dryline (e.g., Anthes et al. 1982; Benjamin 1986; Benjamin and Carlson 1986; Sun and Wu 1992; Ziegler et al. 1995; Shaw et al. 1997). From these numerical studies, it has been also diagnosed that given favorable synoptic conditions, the dryline forms not only due to horizontal gradients in soil moisture and vegetation, but also due to the presence of sloping terrain and vertical shear resulting in regional circulations that are clearly frontogenetic for water vapor.

The original inland sea-breeze hypothesis proposed that weak vertical motions take place mainly on broad horizontal scales of ~100 km, although Sun and Ogura (1979) noted that vertical motions at the dryline could be strongly underestimated through aliasing of the fine-scale gradients onto a large-scale grid. More recent high-resolution observations have indeed revealed that intense vertical motions take place on far smaller scales. For example, Parsons et al. (1991), Zeigler and Hane (1993), and Atkins et al. (1998) found narrow (1–3 km) updraft cores and strong vertical motions that exceeded 4 m s^{-1} in the Parsons et al. (1991) study. Recently simulations (Zeigler et al. 1997) using a nonhydrostatic mesoscale model with a 1-km horizontal grid have reproduced this strong ascent in a narrow band in the vicinity of the dryline interface. The mesoscale ascent near the dryline was shown to be crucial in producing conditions that are locally more favorable to the formation of deep convection (e.g., Ziegler et al. 1997; Ziegler and Rasmussen 1998).

In contrast to these numerous studies of the dryline when the flow responds to surface heating, far fewer investigations have been conducted on the evolution of the nocturnal dryline and how convection is initiated at the dryline during the night. This present study addresses the structure of a nocturnal dryline with special observations over west Texas on 12–13 May 1985, including serial rawinsonde ascents, ground-based Doppler lidar, and other in situ and remote sensors. We will compare our results to the behavior of the dryline during the day and discuss our findings in the context of the diurnal cycle of the dryline and associated regional circulations. The measurements for the present study were taken at the National Weather Service Office in Midland, Texas, as part of the Texas Frontal Experiment (TEXEX). The goals of TEXEX were to examine the short-term (<6 h) evolution of mesoscale preconvective conditions over west Texas. TEXEX was carried out by the National Oceanic and Atmospheric Administration's (NOAA) Environmental Technology Laboratory (formerly the Wave Propagation Laboratory) from 15 April to 31 May 1985. The experimental design and previous results were discussed in Neiman et al. (1988) and Parsons et al. (1991).

Since severe convection developed as a weak cold front approached the dryline from the west, we will also relate our findings to the understanding convective initiation during the night and forecasting severe convection over this region. Previous studies have long shown that convection frequently develops as cold fronts approach the dryline (e.g., Rhea 1966; Koch and McCarthy 1982; Ogura et al. 1982; Shapiro 1982; Schaefer 1986; Doswell 1987; Neiman and Wakimoto 1999; Koch and Clark 1999). The study by Shapiro (1982) first coined the phrase *dryline–frontal merger* to describe the situation when a cold front encounters a dryline and moves into the moist air mass. We will document in the present case how the merger process rapidly (~1–2.5 h) decreased the convective inhibition and increased both the convective instability and the vertical shear of the horizontal wind so that the stable environment changed to one conducive to severe convection.

2. Observational systems and experimental design

TEXEX utilized both remote and in situ meteorological instrumentation. Measurements taken by a dual-channel radiometer (Hogg et al. 1983) provided vertically integrated values of water vapor and liquid water, and a Doppler lidar (Post and Neff 1986) determined the wind field in clear air. The Doppler lidar was scanned primarily by varying the elevation angle through 180°, while maintaining a fixed azimuth angle (commonly called range–height indicator, or RHI, scans). In general, these RHI scans were oriented so that the azimuth angle was approximately perpendicular to the dryline. The

RHIs were interspersed with plan-position indicator (PPI) scans in which the lidar was scanned through 360° in azimuth, while the elevation angle was held fixed.

Our study also used conventional surface and upper-air synoptic data. The conventional upper-air network was supplemented with serial rawinsonde launches at Midland, Texas. Our surface analyses for this study depict dewpoint depressions, since it has long been known that there is a significant gradient in dewpoint temperature across the dryline. We also present surface analysis of virtual potential temperature (θ_v), since it is proportional to density. The values of θ_v were calculated from the reported station temperature, dewpoint temperature, and sea level pressure. In this calculation, the station pressures were derived from the reported ''sea level'' pressure and the actual station temperature, dewpoint temperature, and elevation. A discussion on the accuracy of this method can be found in Parsons et al. (1991). More detailed discussions on the analysis of surface data over sloped terrain can be found in Sangster (1987).

3. Synoptic overview

The detailed measurements of the nocturnal dryline were taken from the evening of 12 May until the early morning hours on 13 May 1985. Figure 1a presents an analysis of temperature and geopotential height at the 850-hPa level for 1800 central standart time (CST) on 12 May. In this analysis, moist south-southeast flow covers most of eastern and central Texas and Oklahoma, with dry southwesterly flow in the range of 15–25 m s^{-1} over and to the west of the experimental site at Midland. At the 850-hPa level, there is also a broad region of relatively low geopotential heights centered over eastern New Mexico (Fig. 1a) with a cold front trailing across the state (see Fig. 2). At this time, the flow at 500 hPa over Texas (Fig. 1b) is strong and with a westerly component. There are considerable wind variations at 500 hPa across the state of Texas with the highest winds located just upstream of the experimental site. A trough at 500 hPa lies to the west of the low pressure center at 850 hPa.

The evolution of the surface conditions after 1800 CST are evident in the wind observations and the analyses of dewpoint depression at three-hourly intervals beginning at 2100 CST on 12 May 1985 (Figs. 2 and 3, respectively). The dryline is identified by a sharp gradient in dewpoint depression meandering approximately north–south through the region at 2100 CST on 12 May and 0000 CST on 13 May (Figs. 2a and 2b) denoting the transition from moist air with a generally southeasterly component to dry southwesterlies. In this case, there is a slight westward movement of the dryline past the experimental site at Midland between 2100 CST on 12 May (Fig. 2a) and 0000 CST on 13 May (Fig. 2b). The westward movement of the dryline at night is typically termed retrogression and is a part of the diurnal cycle of the dryline (Schaefer 1974a,b).

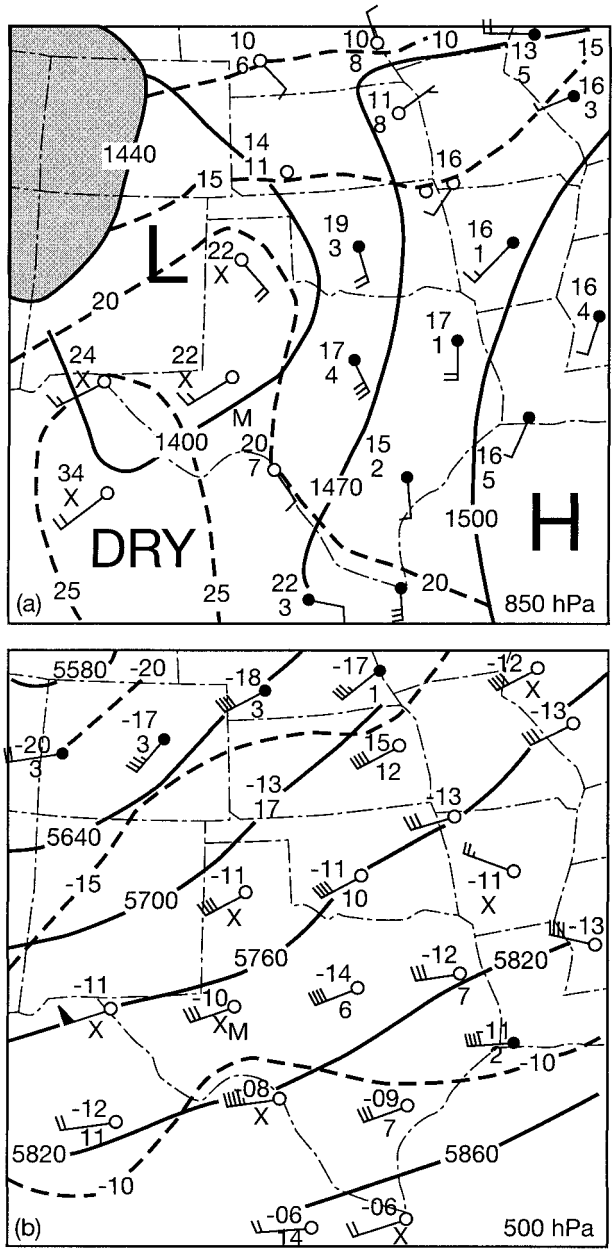

FIG. 1. The (a) 850- and (b) 500-hPa upper-air data and analysis of the height and temperature field at 1800 CST 12 May 1985. The station data, including winds, temperature, dewpoint temperature depression, and cloud cover, are presented in standard meteorological convention. The letter M indicates the location of the experimental site at Midland, TX. The shaded area at 850 hPa indicates the approximate locations where the ground is higher than the 850-hPa level.

The dewpoint depressions are typically small and relatively uniform on the moist (eastern) side of the dryline. The θ_v field, however, is relatively nonuniform with lower values of θ_v over northern and eastern Texas (Fig. 3). The lower values of θ_v over northern Texas are associated with previous convective activity and remain identifiable during the entire analysis period. Across the

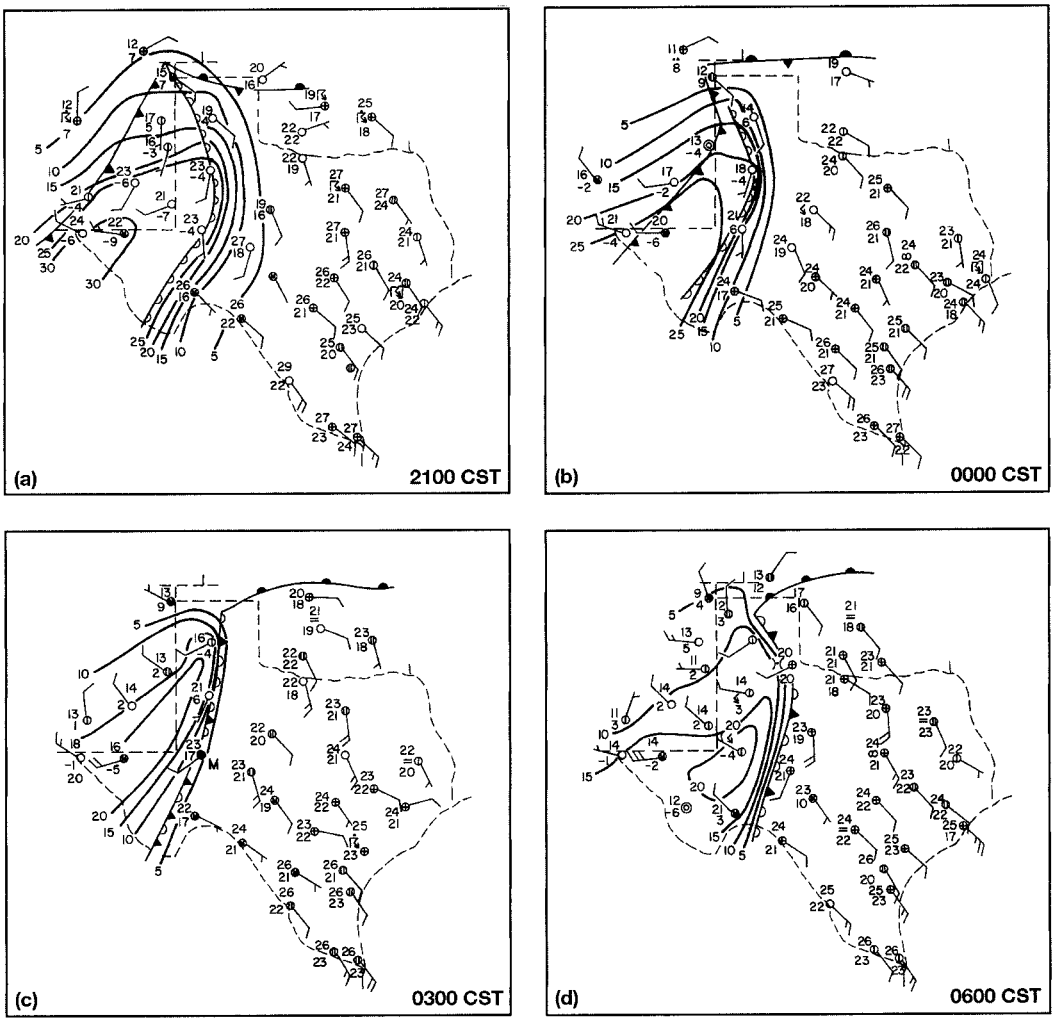

FIG. 2. Surface weather depictions showing temperature, dewpoint temperature, cloud cover, winds, and current weather. Conventional meteorological symbols are used. Frontal (denoted with standard symbols), dryline (denoted by a scalloped line), and dryline–frontal merger (combination of cold frontal and dryline symbols) positions and analyses of dewpoint depressions are also shown. Analyses are at (a) 2100 CST 12 May 1985, and (b) 0000, (c) 0300, and (d) 0600 CST 13 May 1985. The large letter M in (c) denotes the location of the experimental site at Midland.

remainder of the state there is a general east–west gradient. It is this gradient that intensifies in response to differential surface heating to alter the characteristics of the dryline during the afternoon and early evening (see, e.g., Fig. 9 of Parsons et al. 1991). A wedge of very high θ_v to the west between the dryline and a weak cold front is also evident in Fig. 3. The postfrontal air mass also has very large dewpoint depressions (Figs. 2a and 2b).

During this period [2100–0600 local standard time (LST)], a cyclonic circulation at the apex of the dry wedge propagated to the north of the experimental site passing from eastern New Mexico to northern Texas. From the evolution of the surface winds, it is evident that the cyclonic circulation center was a broad feature in eastern New Mexico at 2100 CST on 12 May 1985 that became better defined with time. The surface pressure field (not shown) confirmed that the low pressure center was deepening with time. During this cyclogenesis process, the surface fronts were also becoming better defined. As the cold front approached the dryline from the west, the dry air mass was occluded as the front merged with the dryline sometime near 0300 CST on 13 May 1985 (Figs. 2c and 3c) in a process termed the frontal–dryline merger (Shapiro 1982). In the present case, the frontal–dryline merger slowly moved toward the east (Figs. 2d and 3d) and is designated with a combination of the cold frontal and dryline symbols after the merger. The surface wind direction changes from southeasterly to a direction more parallel to the merger at several stations in the moist air just ahead of the advancing front.

Significant convective weather developed as the merged dryline–cold frontal boundary moved to the east

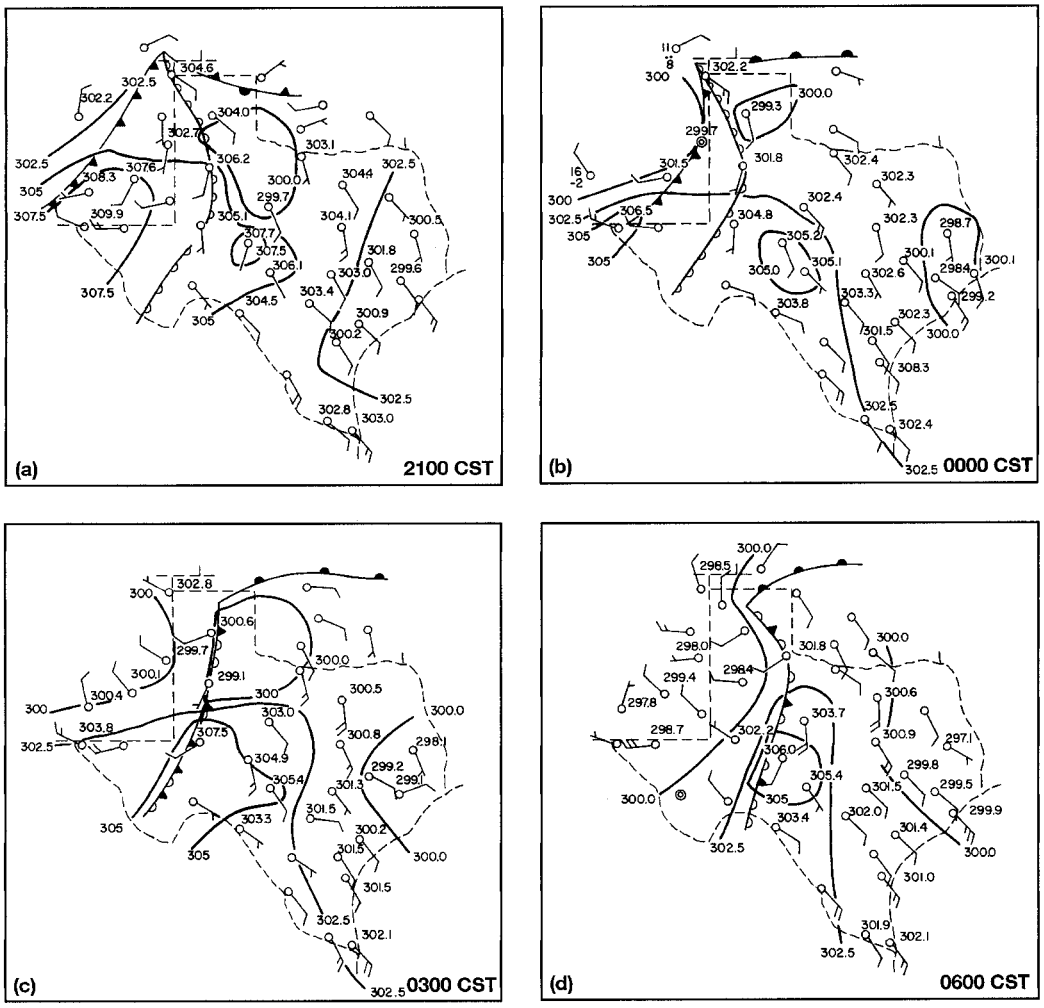

FIG. 3. Surface analysis depicting surface winds and θ_v are shown along with an analysis of θ_v for (a) 2100 CST 12 May 1985, and (b) 0000, (c) 0300, and (d) 0600 CST 13 May 1985. Note that stations in north Texas throughout this period and in Oklahoma near the position of the stationary front in (a) are clearly influenced by deep convection.

(Figs. 2d and 3d). Severe weather caused extensive property damage and numerous injuries, particularly in the vicinity of the suburbs of Dallas, Texas. The radar summaries for the development of this convective event are shown in Fig. 4. These summaries show rapid convective development between 0235 and 0435 CST as the convection develops from a single echo to a solid line of echoes with tops reaching to 17 and 18 km in less than 2 h. More active convection occurred in the southern extent of the line where the higher values of θ_v were evident in Fig. 3.

A series of infrared satellite images (Fig. 5) provides further insight into the initial development of the deep convection. At 0149 CST, there is early evidence of the development with a narrow line of shallow clouds aligned nearly north–south just to the west of Midland (Fig. 5a). From our surface analysis, we speculate that this narrow line of clouds is likely located at the leading edge of the cold front. These narrow rope clouds have been noted by numerous studies to be indicative of strong low-level ascent with advancing cold fronts (e.g., Shapiro et al. 1985). At 0219 CST, there is evidence of a single cell of deep convection (Fig. 5b) that continues to intensify as evidenced in the image at 0249 CST (Fig. 5c). Convection continues to deepen until a convective line is evident at 0349 CST (Fig. 5d). This development in the satellite depiction is consistent with the radar summary between 0235 and 0435 CST (Fig. 4). A severe storm warning noted at ~0300 CST after the convection intensified into a squall line. In our postanalysis, precursors to the formation of deep convection are evident several hours before the warning was issued. These precursors included the existence of high-θ_v air over south-central Texas (see Fig. 3a at 2100 CST 12 May), the intensification of the cyclone and associated cold front after 2100 CST (Figs. 2 and 3), and the presence

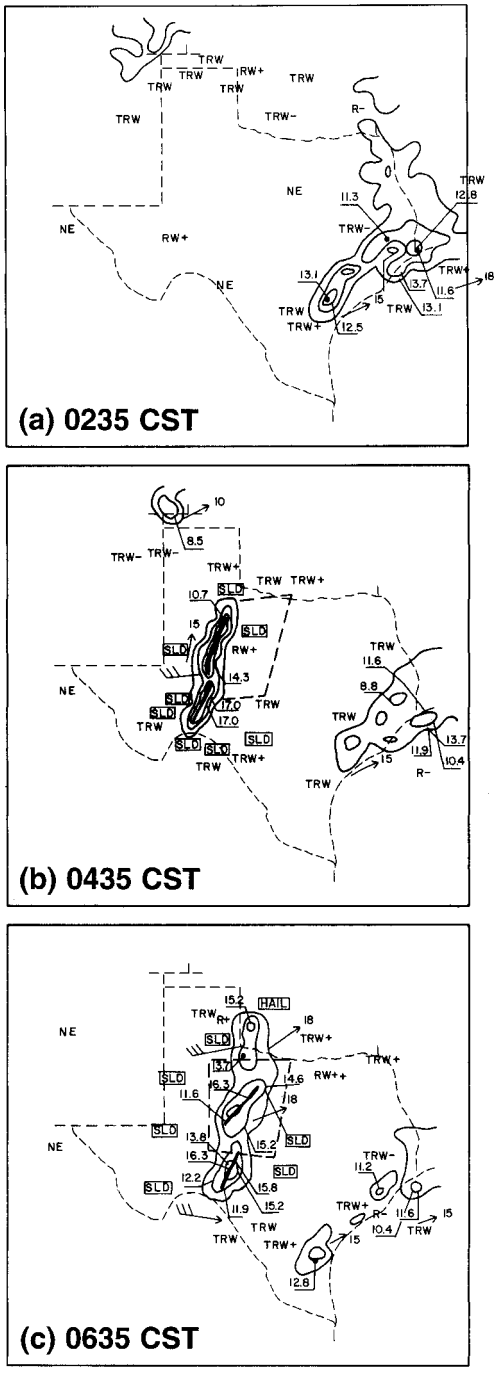

FIG. 4. National Weather Service radar summaries at (a) 0235, (b) 0435, and (c) 0635 CST 13 May 1985. The depictions are in standard convention with the echo tops presented in km.

of a narrow cloud band near the leading edge of the front (Fig. 5a).

4. Special measurements taken at Midland

After setting the stage by describing the synoptic situation over the region, we will now concentrate on time series measurements taken at the experimental site at Midland. A series of rawinsondes were released beginning at 2100 CST on 12 May 1985 (Fig. 6). The first sounding (Fig. 6a) is clearly on the west or dry side of the dryline boundary, with its characteristic deep and dry boundary layer. The dryness evident in the sounding is consistent with the surface analyses (Figs. 2 and 3), which depict the dryline to the east of Midland at 2100 CST. There is no convective available potential energy (CAPE) in this sounding. The sounding at 2335 CST on 13 May (Fig. 6b) shows that pronounced changes occurred in the boundary layer after the passage of the retrogressing dryline as the boundary layer moistened, the temperature cooled, and the lapse rate stabilized. The cooling may have resulted from either horizontal advection or nocturnal radiational cooling. A low-level jet is evident in the moist air mass between 800 and 900 hPa, with the highest moisture content near the height of the low-level jet. We will term this feature the low-level jet as past studies use this phrase for this feature. We do admit, however, that we do not have any detailed information on the lateral structure of the jet. This sounding is slightly unstable with a CAPE of 524 J kg^{-1}. However, since ~412 J kg^{-1} of energy (termed convective inhibition) is required for a parcel to reach its level of free convection, it is unlikely that deep convection will be initiated.

After 2335 CST, moistening of the boundary layer continued with near-saturated conditions just below the axis of the low-level jet as evidenced by the sounding at 0216 CST on 13 May 1985 (Fig. 6c). The moistening extended to a depth of nearly 700 hPa between the 2335 and 0216 CST soundings with cooling also observed near the 700-hPa level. These changes result in the CAPE increasing dramatically to 3417 J kg^{-1} while the CIN drops to -9 J kg^{-1}. There is also a dramatic strengthening of the winds near and above ~500 hPa (Figs. 6b and 6c). The bulk Richardson number for the sounding at 0216 CST is ~29. The magnitudes of the CAPE and the bulk Richardson number at this time fall within the range for severe supercell convection. The very dry sounding at 0500 CST on 13 May 1985 in Fig. 6d was taken after the passage of the cold front and the associated convective system.

The time series of vertically integrated water vapor and liquid water are shown together with the surface observations in Fig. 7. The retrogression of the dryline past Midland coincided with a steep increase in the integrated water vapor after 2200 CST. However, the dominant feature of the time series is a more gradual increase in the water vapor from 1.0 to 3.5 cm that took place after the dryline passage in the 4 h from ~2200 CST to ~0200 CST. An even more rapid decrease was observed after the passage of the dryline–frontal merger. The general increase in the integrated water vapor coincided with the moistening of the soundings below ~700 hPa. The surface dewpoint (Fig. 7) showed relatively little change at the time of the dryline passage

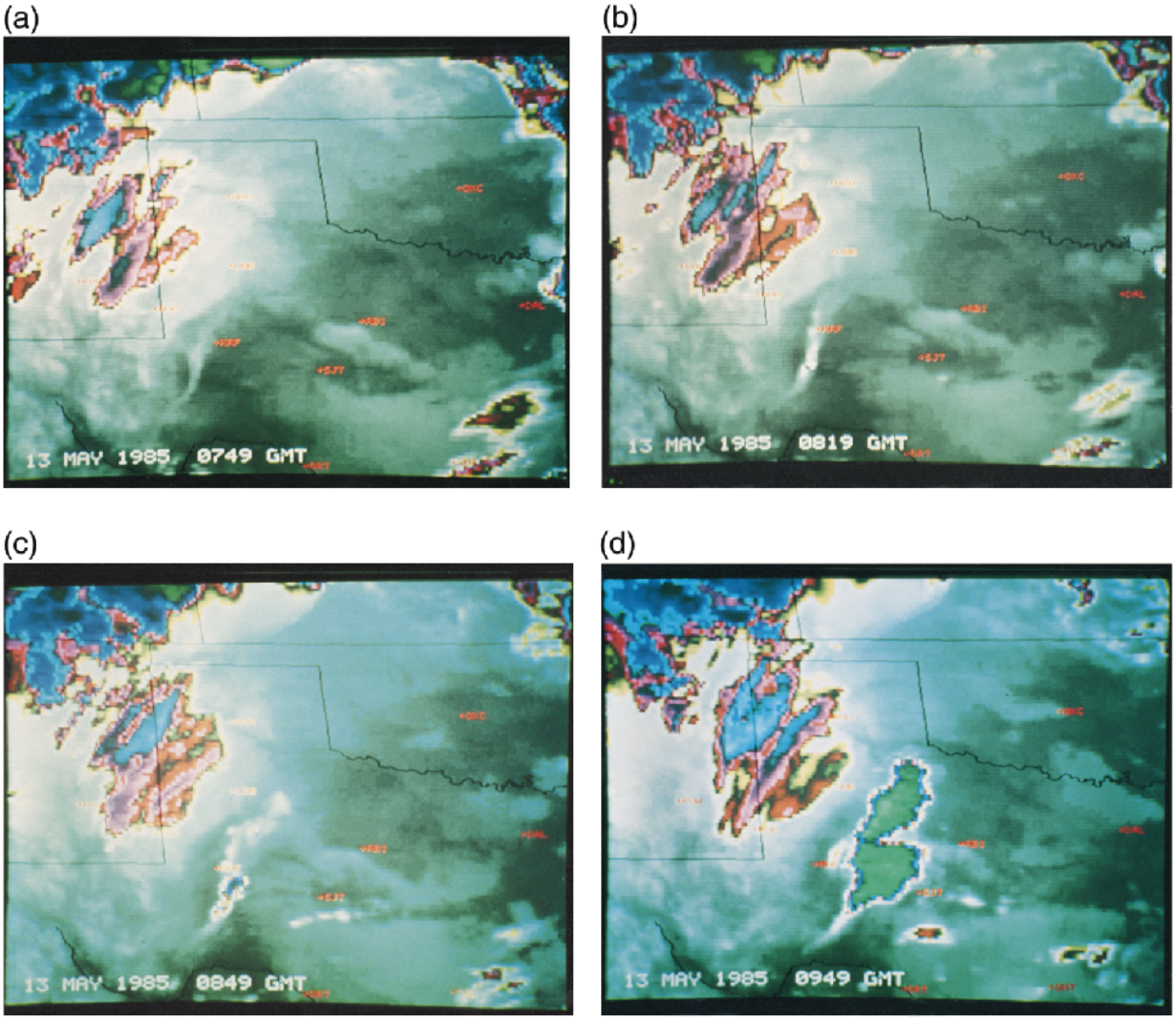

FIG. 5. A series of infrared satellite images color enhanced at (a) 0149, (b) 0219, (c) 0249, and (d) 0349 CST 13 May 1985. The temperature scale has been enhanced to better reveal the areas of deep convection.

for the nocturnal case, other than a continuation of the slow increase in dewpoint temperature with time. Largest increases in the surface dewpoint took place 2–4 h after the dryline passage. The behavior of the surface dewpoint is consistent with the earlier soundings showing moisture being advected at the level of the low-level jet (Figs. 6b and 6c). The measurement of vertically integrated liquid water (Fig. 7) indicates that cloud formed at ~0200 CST on 13 May with clouds of more significant liquid water evident at ~0230 and ~0315 CST.

Doppler lidar measurements were taken as the dryline retrogressed past Midland. PPI scans at an elevation angle of 10° were taken both prior to and following the arrival of the dryline. The PPI ahead of the dryline at 2142 CST (Fig. 8a) reveals generally deep southwesterly winds both in the shape of the 0 m s^{-1} line, which can be used to infer wind direction (i.e., Baynton et al. 1977), and in the locations of the maximum wind speeds. A PPI taken at 2235 CST (Fig. 8b), after the arrival of the moist air, indicates that the arrival of the moist air coincided with a low-level jet consistent with the rawinsonde data presented earlier. At 2235 CST, the low-level jet was from the south-southwest in excess of 18 m s^{-1} at a height of ~530 m. The shape of the 0 m s^{-1} line at this time suggests that the wind direction veers above the jet axis so that the flow above ~1.3 km is again southwesterly. The change in the shape of the 0 m s^{-1} line to the NW between 8 and 12 km in range is the PPI scan intersecting with the leading edge of the dryline.

An RHI scan taken at 2211 CST and oriented SE–NW is displayed in Fig. 9a. In this depiction, the source of the moist air is on the right side of the figure, the dryline interface is denoted with a solid white line, and the direction of the radial velocities at lower levels is

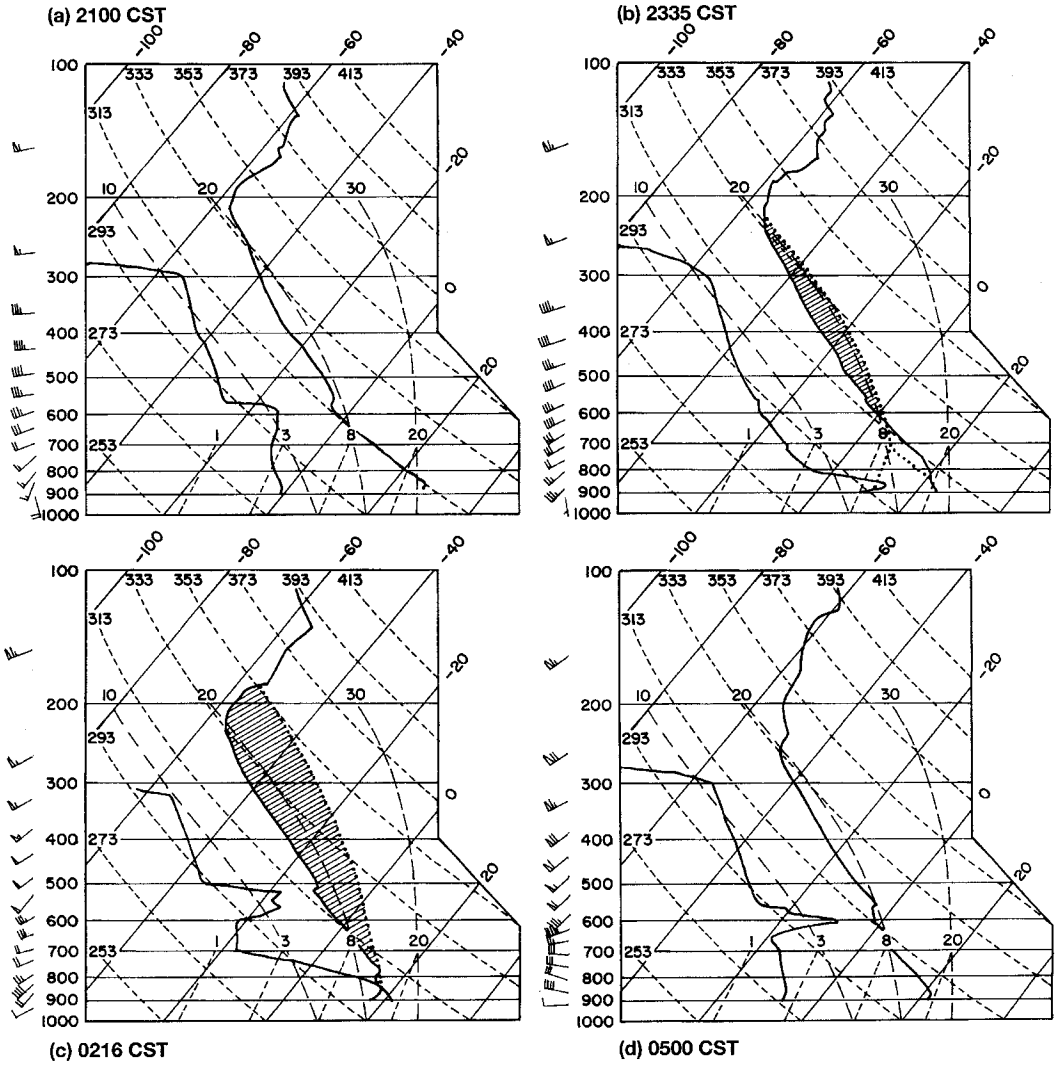

FIG. 6. Data from serial rawinsonde ascents launched from Midland by the National Weather Service. The launch times are approximately (a) 2100 and (b) 2335 CST 12 May, and (c) 0216 and (d) 0500 CST 13 May 1985. The data is displayed on a skew *T* plot using conventional notations for the wind speed and direction. The parcel ascents utilized to derive the CAPEs are also shown for (b) and (c).

indicated with arrows. The RHI indicates that the moist air behind the dryline is moving toward the NW at ~7–9 m s^{-1}. A thin layer of weak return flow is evident above the dryline interface (Fig. 9a). Alternating layers of flow aloft toward (~2–4 km) and away from the dryline (4–5 km) are consistent with the general increase in the wind speed with height in the sounding data (Fig. 6) and in the lidar PPIs (Fig. 8b). The slope of the interface is relatively gentle, with the depth of the moist air increasing by 1 km over ~15 km in horizontal distance. Locally, however, the slope can vary significantly. For example, between 4.0 and 6.0 km in range east of the lidar in Fig. 9a there is a local steepening of the velocity contours.

These local bulges in dryline depth seem to have some spatial coherence and a northerly component of movement, although it is difficult to establish from a single Doppler lidar, since only one component of the wind is measured. The relatively short range of the lidar also made it difficult to study these features in more detail. However, some inferences could be made about the behavior of these bulges, such as evidence that these features were sometimes associated with decreases in vertical shear across the interface and flow reversals within the moist air. A flow reversal is illustrated in the RHI taken at 2226 CST (Fig. 9b), when a bulge is located toward the northwest of the lidar with weak WNW flow underneath the local steepening. While we do feel that vertical mixing is likely, perhaps from breaking waves, and may explain the changes in the shear (not shown) and the flow reversals, we cannot be certain without corresponding thermodynamic data. We do note that

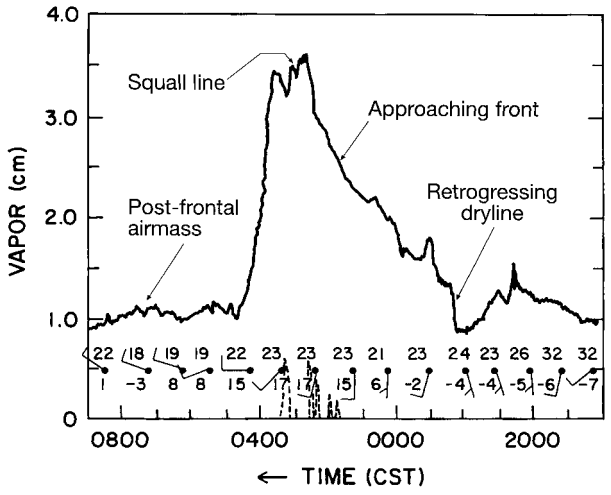

FIG. 7. Column-integrated values of water vapor as a function of time measured by the radiometer on 12–13 May 1985 at Midland. The hourly surface observations of wind, temperature, and dewpoint temperature are plotted above the water vapor trace. An increase in water vapor is evident when the dryline retrogressed past Midland after 2200 CST 12 May 1985. Liquid water measurements are also shown with the dashed line. Significant synoptic events are labeled.

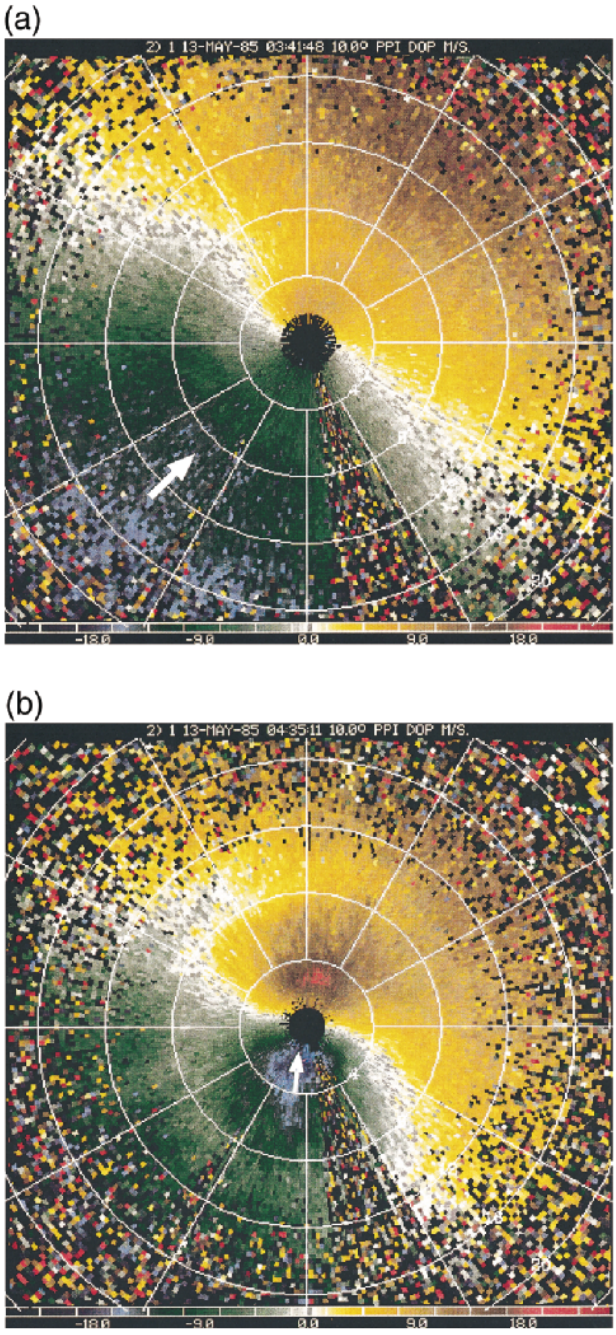

FIG. 8. Horizontal cross sections of radial velocity measured by the Doppler lidar in PPI display mode at an elevation angle of 10°. The color code in the lower portion of the figure is in m s^{-1}. PPI taken from Midland at (a) 2142 and (b) 2235 CST 12 May 1985. The arrows indicate the direction of the maximum radial velocities. In (b) the arrow indicates the low-level jet.

waves appear to be a common feature along dryline interfaces (see McCarthy and Koch 1982; Schaefer 1986; Parsons et al. 1991; Crawford and Bluestein 1997). Coulter (1990) also presented evidence for vertical mixing in nocturnal environments leading to thermodynamic changes at the surface. In the present case, the vertical shear below the low-level jet axis, or the shear between the jet and the flow within the dry air aloft, might be sufficient to lower the Richardson number and excite shear-induced mixing or waves. The bulk Richardson number calculated for the soundings taken at 2335 and 0216 CST was ~0.4 to 0.6 for the layer below the axis of the low-level jet with values below 0.25 observed when the individual 30-s sounding data points (~150 m apart in height) were utilized in the calculation. These relatively low Richardson numbers support the hypothesis that shear-induced processes may have been responsible for the observed bulges and subsequent mixing.

The bulges and regions of flow reversal also gave the dryline the appearance of an irregular movement westward and an irregular orientation. Unfortunately, the resultant nonsteadiness and three-dimensionality prevented the calculation of vertical motions by the two-dimensional technique used in an earlier study of a late afternoon/evening dryline observed during TEXEX with the same instrumentation (Parsons et al. 1991). However, qualitative comparisons can be made between the two cases. For example, the early evening dryline in the Parsons et al. (1991) study was characterized by rapid wind and moisture changes at the surface. For the nocturnal event, the moisture changes were instead most readily evident aloft near the axis of the low-level jet. The westward advection of the moisture by the jet in the present case is consistent with the inertial oscillation of the jet (e.g., Bonner 1968; Parish et al. 1988). The westward propagation of the dryline observed in the current case also confirms the advective nature of the

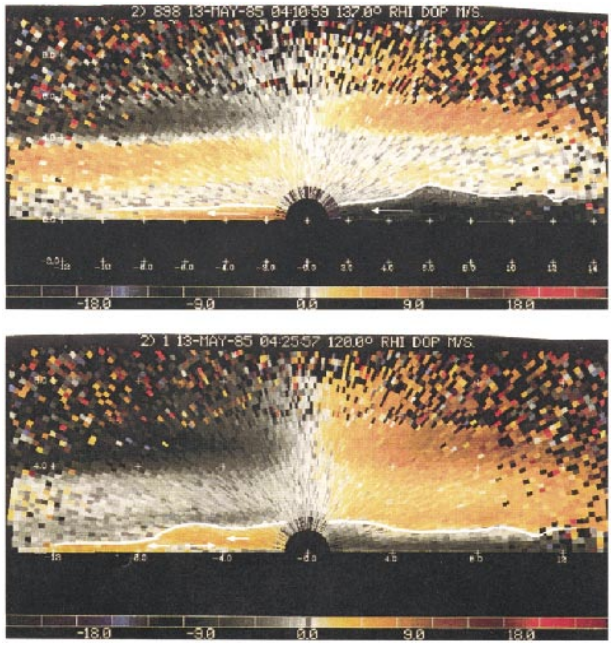

FIG. 9. Vertical cross sections of radial velocity measured by the Doppler lidar in RHI display mode. The color code in the lower portion of the figure is in m s^{-1}. (a) An RHI taken at 2211 CST 12 May 1985. The display is oriented approximately NW–SE (137°–317° in meteorological coordinates with 90°–180° as east–west). (b) An RHI taken at 2227 CST 13 May 1985. The horizontal component of the measured radial velocity is indicated with the arrows. This display is oriented 120°–300°. The scan angles were selected to be approximately perpendicular to the dryline. The determination of the orientation was difficult because, as mentioned in the text, the dryline was not two-dimensional and the movement was irregular.

nocturnal dryline (Schaefer 1974a,b; 1986), although these studies did not specifically link the advection to the evolution of the jet. Also, in contrast, to the steep, near-vertical slope of the dryline in studies of afternoon and early evening systems, this nocturnal dryline had a gentle slope near its leading edge. As noted earlier, McCarthy and Koch (1982) also observed steeper, near-vertical dryline interface during the afternoon.

The smaller slope of the nocturnal interface, for example, together with the weaker confluence in the flow components normal to the dryline, suggests that this nocturnal dryline has smaller vertical motions than was found in recent investigations of the afternoon/early evening dryline. A crude estimate of several 10 cm s^{-1} can be obtained for the vertical motion of the dry air riding over the dryline in the present nocturnal case. This estimate was obtained from the slope of the dryline and the relative flow above the dryline shown in Fig. 9. The vertical motions in the present case contrast with the updrafts of several meters per second updrafts observed in the previously studied afternoon/early evening cases. Perhaps the most important difference between the dryline structures found in the nocturnal and late afternoon cases is that the nocturnal case lacks the local deepening of the moist air at the leading edge of the dryline caused by lifting of the moist air near the leading edge of the dryline. This deep lifting of the moist air is in part what makes the afternoon/early evening dryline a relatively favorable location for the initiation of deep convection. We hypothesize from the present case that the circulations inherent to the shallower dryline at night are far less favorable for the initiation of deep convection.

During the afternoon and early evening, the lifting results from the convergence of moist upslope flow driven in part by differential heating with a deep, dry boundary layer where the westerly component of the winds have often increased through the entrainment of high momentum air from aloft. The magnitude of the density gradient across the dryline in afternoon induced by differential heating has been investigated by a number of studies (Fujita 1958; Parsons et al. 1991; Zeigler and Hane 1993; Wakimoto et al. 1996; Crawford and Bluestein 1997; Shaw et al. 1997; Atkins et al. 1998). One can infer from these studies that the frontogenetic character of the flow can sometimes extend beyond the moisture field to θ_v, with the afternoon and early evening dryline characterized by observable mesoscale and local gradients. The mesoscale gradients in density are relatively weak, however, suggesting that the conceptual model of a density current may often at best generally only be applicable near the dryline interface (Crawford and Bluestein 1997; Atkins et al. 1998). For this nocturnal event, a surface gradient in density (θ_v) was not present near the time of the dryline passage as the daytime gradient decreased due to the dry air cooling more rapidly at night due to radiational effects (not shown).

The Sun and Wu (1992) idealized modeling study also predicts a change in the slope of the dryline as differential surface heating produced a local gradient in density across the dryline with a steep vertical slope in the afternoon, while the dryline had a more gentle slope during the late night and very early morning hours. The simulations of Sun and Wu (1992), however, indicate that a relatively strong gradient is maintained at night. They note that ''the moisture gradient is a maximum around midnight'' and ''the strong moisture gradient was also sustained at night by low-level convergence.'' From this point of view, one might expect the dryline to remain an area that is favorable to the initiation of convection into the late night or even the early morning. This point of view conflicts with the findings from this case and our impression of other events observed during TEXEX in that the dryline is difficult to detect at the surface during the night. Indeed, Ogura et al. (1982) state ''the dryline is no longer identifiable'' in their case study at 0200 CST. Schaefer (1986) also notes that the strength of the moisture gradient tends to be better defined in the midafternoon than during the early morning hours and convergence is maximized in the early evening during retrogression. Further investigations are clearly needed describing the three-dimensional distribution of moisture and mesoscale convergence in the

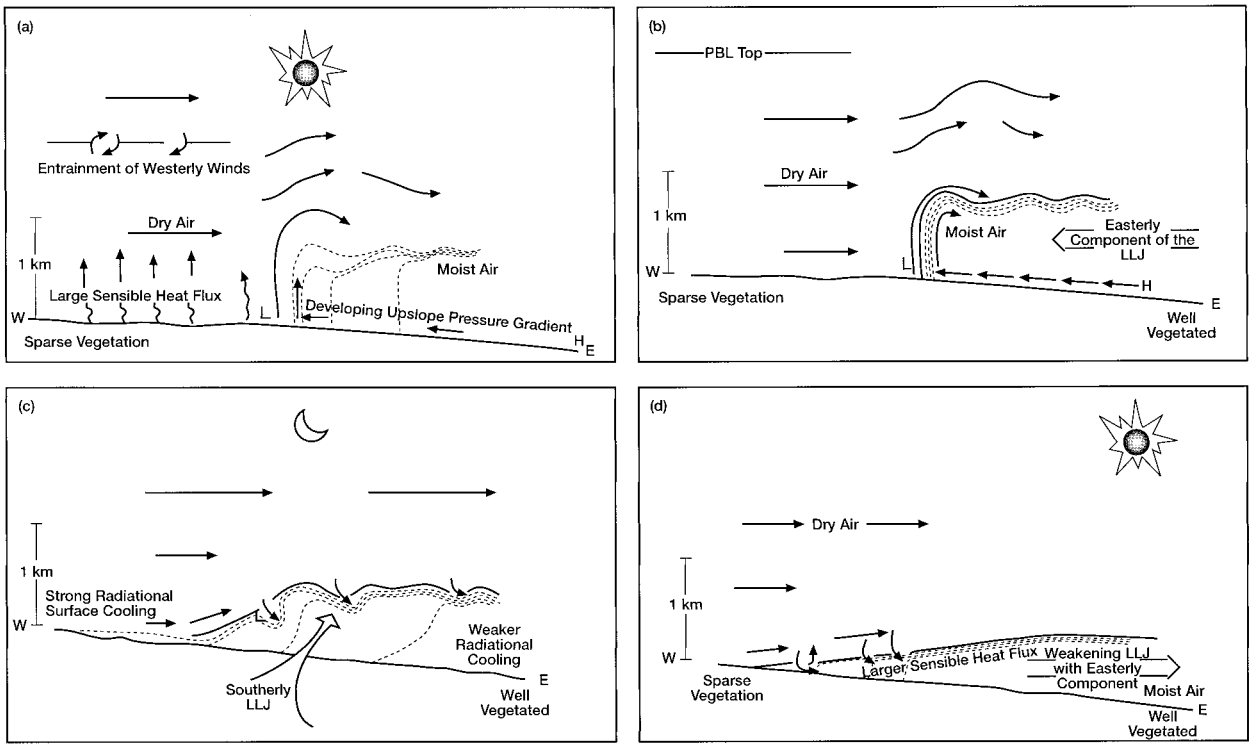

FIG. 10. A schematic of the diurnal evolution of the dryline. The dashed lines indicate lines of constant ratio water vapor mixing. (a) Solar noon: the flow near the dryline interface is strongly frontogenetic for water vapor and weakly frontogenetic for temperature. (b) After sunset: the dryline retrogresses to the east in response to a developed upslope flow and commencement of the easterly winds associated with the onset of the low-level jet (LLJ). (c) Midnight: a more gently sloping dryline interface. The differential longwave cooling makes the dryline more difficult to detect in both the moisture and the thermal fields. (d) After sunrise: vertical mixing in response to surface heating mixes out the nocturnal inversion more rapidly to the west, causing an apparent eastward movement of the dryline (dotted lines).

dryline environment over a diurnal cycle(s) in order to resolve these issues. One possible reconciliation of these viewpoints is that the dryline might be stronger aloft at night as predicted by Sun and Wu (1992), but simply more difficult to detect within the surface layer due to the development of a nocturnal inversion in the dry air mass. It is alternatively possible that the relative strength of the dryline at night may be overestimated in the Sun and Wu study, perhaps due to general difficulties in accurately modeling the type of mixing events in stable boundary layers that we observed in the present case. The results of Sun and Wu might also be different from the past observations due to their idealized initialization or their relatively coarse horizontal resolution.

5. Toward a conceptual model of the diurnal evolution of the dryline

Our nocturnal observations provide further support for a conceptual model of the diurnal variation of the dryline based on differential surface heating and cooling. It should be noted that although a conceptual model is useful for many purposes, significant variations can occur from case to case and region to region, as cautioned by Hane et al. (1993) and Crawford and Bluestein (1997). For example, since surface characteristics are to a large degree responsible for producing gradients in boundary layer thermodynamics, one can expect irregularities to develop in the cross- and along-dryline directions due to subregional surface irregularities and such factors as cloud cover, soil moisture, vegetation, convective outflows, previous rainfall episodes, and spatial variations in the turbulent mixing process. In addition, the spatial relationship between the dryline and other synoptic and regional features, such as the lee pressure trough, can also influence dryline behavior, as cautioned in previous studies. Multiple regions of enhanced gradients can also be present at times, particularly when the dryline occurs on successive days (e.g., Schaefer 1986). Another caution concerning our conceptual model is that there are far more studies of the afternoon and evening dryline than the circulations observed at night or during the morning. It is also possible that the dryline observed in this case was strongly impacted by the frontal ciculations well before the merger process.

Our proposed conceptual model is shown in Fig. 10 with the situation in early afternoon depicted in Fig. 10a. As noted earlier, previous findings generally validate the inland sea-breeze hypothesis. Thus, differential

surface heating will produce a pressure gradient force directed upslope in the early afternoon with weak easterly winds perhaps forming within the moist boundary layer. On the west side of the dryline, downward mixing of gusty dry air from aloft into the deepening boundary layer takes place as the solar heating of the surface progresses. These circulations are frontogenetic for the moisture field and begin to form a well-defined gradient in moisture and perhaps a weak, but significant, local gradient in density. By itself, however, the strength of this density gradient is not a good predictor of vertical ascent at the dryline interface (Zeigler et al. 1995). The inclusion of horizontal vorticity balance (Rotunno et al. 1988) across the dryline might result in a better predictor of vertical motion as Parsons (1992) has shown a strong dependence of the depth and intensity of vertical motions across boundaries even for relatively weak density gradients.

During the evening (Fig. 10b), the dryline often retrogresses westward at a maximum rate with a sharp moisture gradient. This retrogression is due to a number of factors, including 1) rapid nocturnal cooling in the dry air, which decreases the downward mixing on the dry side and causes a corresponding relatively stronger decrease in the wind field in the dry air mass as proposed by Schaefer (1974a,b); 2) the prolonged period of differential heating producing an upslope pressure gradient, resulting in upslope flow in the lower portions of an Ekman boundary layer (Bluestein and Crawford 1997); and 3) a pronounced westward component of the wind in the moist air associated with the directional changes of the low-level jet following the frictional decoupling. Our results suggest the later process. Further evidence includes the observations by Parish et al. (1988), which clearly show that the up- and downslope variations in the wind speed within the moist air are ageostrophic and are largely due to the inertial oscillation of the low-level jet, as proposed by Blackadar (1957). The diurnal variation in the pressure gradient, in contrast, is mainly responsible for the geostrophic behavior of the wind. The Arritt et al. (1997) study also shows that 850-hPa ageostrophic easterly winds are large at this time of day in low-level jet situations.

As the diurnal cycle progresses (Fig. 10c), the low-level jet within the moist air mass typically turns toward a more southerly direction, parallel to the dryline, and the upslope pressure force associated with the gradient in surface heating found during the day will no longer be present. Vertical mixing may also decrease this density difference. The more rapid cooling on the dry side may even begin to produce a pressure gradient that is directed downslope (e.g., Holton 1967; Parish et al. 1988), decelerating the westerly component and perhaps eventually producing weak downslope flow and an advection of moisture to the east. In our conceptual model, we therefore propose that the dryline will slow and eventually stop its westward progression as the night progresses. As in the present case, the sloped nature of the dryline appears well before any reversal in the density gradient so that the analogy of the dryline to a warm front is strictly speaking not correct.

An implication of the dryline being less steep at night is that the moist air becomes far shallower over the higher elevations to the west. Thus, over the higher terrain, surface heating in the morning (Fig. 10d) will tend to more rapidly mix the low-level moist air with dry air aloft, giving the appearance of an eastward-moving dryline. This idea was first put forth by Schaefer (1974a,b), subsequently found in the simulations (e.g., Sun and Wu 1992), and implied in the observations by Hane et al. (1993). This process explains the tendency for the ''movement'' of the dryline to be inconsistent with horizontal advection during the morning. However, since the inertial oscillation of the low-level jet will begin to produce a westerly wind component during the early morning hours, and the cooling on the sloped terrain will also force eastward accelerations, it is likely that some eastward advection of the low-level moisture may also take place prior to and just following sunrise. In our conceptual model, convection is most likely to be generated near the dryline interface in the afternoon and early evening, rather than late at night and in the morning as the moisture is locally deeper and the convergence stronger. Future studies will show whether our proposed conceptual model is valid as we only studied one nocturnal case and it was influenced by the approaching cold front.

6. Implications for the initiation of deep convection

While the circulations at the dryline interface seem less likely to generate convection at night, convection did develop at night in this case as a cold front merged with the dryline. We will discuss several aspects of the observed dryline–frontal merger in the context of convective initation. First, we note that several previous studies (Koch and McCarthy 1982; Shapiro 1982; Doswell 1987; Trier et al. 1991; Neiman and Wakimoto 1999) showed how secondary circulations associated with the front produced mesoscale ascent within the moist air mass ahead of the cold front over the Great Plains. The ascent results in a deepening of low-level moisture ahead of the front producing an environment more favorable to deep convection. In the present study, a dramatic increase within 2.5 h was noted in the CAPE with a similar decrease in convective inhibition. The nature of our measurements made at a single site make it difficult to compare our observations to the aircraft traverses in the Shapiro (1982) and Neiman and Wakimoto (1999) studies. In order to make this comparison, we constructed a vertical cross section of moisture from our data using the serial rawinsonde ascents supplemented with the integrated water vapor measurements as a subjective constraint. The resulting cross section is shown in Fig. 11a. A vertical cross section of water

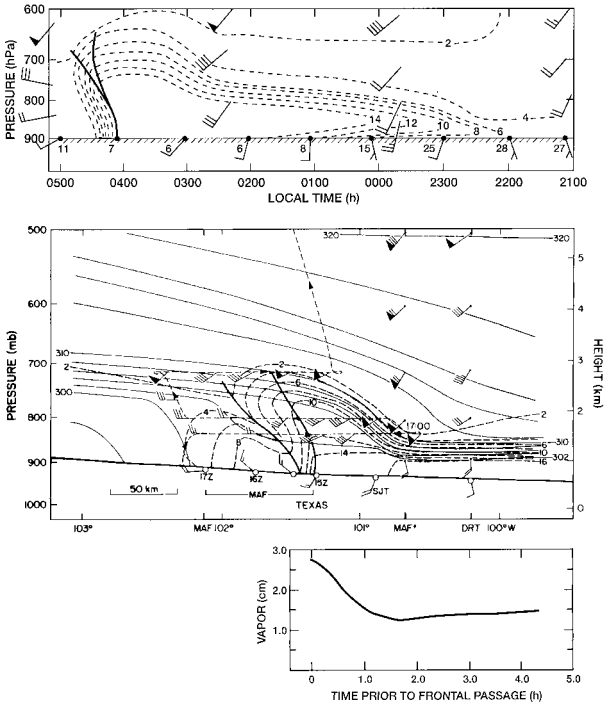

FIG. 11. A vertical cross section of moisture mixing ratio (g kg^{-1}) and wind speed and direction (conventional notation) through a dryline–frontal merger on 13 May 1985. The cross section was constructed from the serial rawinsonde ascents shown in Fig. 6. Hourly surface station data are also shown. (b) A vertical cross section of potential temperature (K, solid line), moisture mixing ratio (g kg^{-1}), and wind speed and direction (conventional notation) through a dryline–frontal merger adapted from Shapiro (1982). A time-to-space conversion was used to represent conditions at 1100 CST 3 Apr 1981. The integrated water vapor time series constructed from the cross section is also shown using a space-to-time conversion.

vapor from the Shapiro (1982) study and a time trace of vertically integrated water vapor derived from the cross section are shown in Fig. 11b. The deepening of the moisture just prior to the arrival of the front and the increase in vertical shear are evident in both cases. The timescale of the destabilization by mesoscale ascent in the Shapiro (1982) study was ~1 h. We earlier estimated a timescale of less than ~2.5 h as the destabilization occurred between the 2335 and 0216 CST soundings. From the constrained vertical cross section constructed for the present case (Fig. 11a), we note a further deepening of the moisture occurs within ~1 h of the frontal passage due to a correspondingly steep increase in the vertically integrated water vapor. The local deepening of the moisture appears similar to the deepening caused by secondary circulations in the Shapiro (1982) study of a morning case (Fig. 11b) and in the other cases discussed earlier. Thus, the dramatic stability changes in the present case likely result from the retrogression of the dryline and the secondary circulations ahead of the dryline–frontal merger.

Recently, however, Koch and Clark (1999) showed that secondary circulations and direct frontal lifting alone may not accurately describe the initiation of convection during the merger process. In the Koch and Clark (1999) study, lifting ahead of the front may also be due to the formation of a bore that develops as the front moves into the moist air mass. The destabilization in the Koch and Clark (1999) study occurs even more rapidly (~30 min). We cannot detect these local changes with the observing network employed in the present study, although the steep increase in integrated water vapor near the time when convection was initiated associated with multiple structures in the vertically integrated liquid water suggest that such a process could not be ruled out.

The increased horizontal resolution of mesoscale models used in research compared to those available at the time of the measurements in this study and the Shapiro (1982) work now provides some possibility of resolving the rapid destabilization caused by bores and secondary circulations. However, relative to the number of observational studies detailing the destabilization process, there is far less information about the performance of numerical models for these situations. These simulations will be a stringent test of a model, since, for example, the nature of secondary circulations and the bores depend on static stability, vertical shear, and the inertial stability. Thus, small errors in the model forecast will directly feedback on the magnitude, depth, and type of the vertical motions ahead of the front. However, even with ''relatively good model forecasts'' it is clear that observations will still play a role in predicting severe weather outbreaks due to possible errors in the timing and location of the frontal systems and their associated wind maxima. To be useful, observations must be able to detect the deepening in the moisture field and the changes in the vertical shear on timescales of ~1 h or less. The vertical shear measurements are currently available from the wind profiler network. Until we have the ability to operationally detect water vapor in a manner analogous to the wind profiler network with an emphasis on moisture levels within and just above the boundary layer, we will need to rely on integrated water vapor measurements. Integrated water vapor measurements, however, are of practical use as evidenced by this study and a conversion of the Shapiro (1982) results to a similar time trace, since thermodynamics dictate that the bulk of the water vapor is located in the lower troposphere. Fortunately, the implementation of low-cost Global Positioning System (GPS) sensors applicable for estimates of vertically integrated water vapor will provide a detailed picture of the water vapor over the continental United States. Some initial work on the use of GPS-integrated water vapor measurements can be found in Businger et al. (1996).

7. Summary of future research needs

This study provides further insight into the nature of the nocturnal dryline and how severe convection can

initiate at night in an environment previously unsuitable for deep convection. We also noted several areas where we believe that our knowledge is lacking. First, we have isolated the need for observational studies of the dryline over several diurnal cycles for validation of conceptual models and high-resolution numerical simulations. Currently, our knowledge of the diurnal variation of the dryline depends on measurements made during different portions of the lifetime of various drylines. These measurements would also address how the strength of the moisture gradient and convergence varies with the diurnal cycle. If the simulations overpredict moisture gradient at night, there is the possibility that more work is needed into how well these models treat stable, nocturnal boundary layers and intermittent mixing events. Another issue is whether the rapid evolution of the water vapor field in this and other studies can be adequately observed with proposed GPS networks measuring integrated water vapor and whether these observations will improve predictions of convective activity and of severe weather. Our analysis suggests that there is the possibility that precursors for convective development should be evident in such datasets. A preliminary data assimilation and forecast experiment with a mesoscale model did show a positive impact of GPS data on the prediction of convective rainfall using a four-dimensional data assimilation system (Guo et al. 2000). Finally, the work by Koch and Clark (1999) raises the issue that the interaction between the front and the dryline is more complex than the simple merger model and their findings suggest that more work is needed to establish the relative frequency of local bore versus frontal lifting events.

Acknowledgments. We especially appreciate the skillful work of our colleagues at the Environmental Technology Laboratory who collected the lidar, radiometer, and rawinsonde data. The cooperation and involvement of the staff at the National Weather Service Office at Midland, Texas, during the TEXEX project are also gratefully acknowledged. We thank Keith Browning, as this work was completed while the lead author was a visitor at the Joint Centre for Mesoscale Meteorology in Reading, United Kingdom. T. Matejka (NOAA/ERL/NSSL) provided the software to calculate the θ_v fields from station data. R. Maddox (NOAA/ERL/NSSL) and F. Sanders (Marblehead, MA) provided extremely helpful comments the very early stages of this research, while encouragement from P. Bannon (The Pennsylvania State University) and R. Smith (University of Munich) led to the writing up of this article. We would also like to thank J. Lukas (NCAR) for an excellent technical review of this manuscript prior to submission. J. Intrieri and Mike Hardesty (both NOAA/ERL/ETL) kindly provided the lidar data. M. Weisman (NCAR) and an anonymous reviewer provided insightful reviews.

REFERENCES

Anthes, R. A., Y.-H. Kuo, S. G. Benjamin, and Y.-F. Li, 1982: The evolution of the mesoscale environment of severe local storms: Preliminary modeling results. *Mon. Wea. Rev.*, **110,** 1185–1213.

Arritt, R. W., T. D. Rink, M. Segal, D. P. Todey, C. A. Clark, M. J. Mitchell, and K. M. Labas, 1997: The Great Plains low-level jet during the warm season of 1993. *Mon. Wea. Rev.*, **125,** 2176–2192.

Atkins, N. T., R. M. Wakimoto, and C. L. Ziegler, 1998: Observations of finescale structure of a dryline during VORTEX 95. *Mon. Wea. Rev.*, **126,** 525–550.

Baynton, H. W., R. J. Serafin, C. L. Frush, G. R. Gray, P. V. Hobbs, R. A. Houze Jr., and J. D. Locatelli, 1977: Real-time wind measurements in extratropical cyclones by means of Doppler radar. *J. Appl. Meteor.*, **16,** 1022–1028.

Benjamin, S. G., 1986: Some effects of surface heating and topography on the regional severe storm environment. Part II: Two-dimensional idealized experiments. *Mon. Wea. Rev.*, **114,** 330–343.

——, and T. N. Carlson, 1986: Some effects of surface heating and topography on the regional severe storm environment. Part I: Three-dimensional simulations. *Mon. Wea. Rev.*, **114,** 307–329.

Blackadar, A. K., 1957: Boundary-layer wind maxima and their significance for the growth of nocturnal inversions. *Bull. Amer. Meteor. Soc.*, **38,** 283–290.

Bluestein, H. B., and S. S. Parker, 1993: Modes of isolated, severe storm formation along the dryline. *Mon. Wea. Rev.*, **121,** 1354–1372.

——, and T. M. Crawford, 1997: Mesoscale dynamics of the near-dryline environment: Analysis of data front COPS-91. *Mon. Wea. Rev.*, **125,** 2161–2175.

Bonner, W. D., 1968: Climatology of the low-level jet. *Mon. Wea. Rev.*, **96,** 833–850.

Businger, S., and Coauthors, 1996: The promise of GPS in atmospheric monitoring. *Bull. Amer. Meteor. Soc.*, **77,** 5–18.

Coulter, R. L., 1990: A case study of turbulence in the stable boundary layer. *Bound.-Layer Meteor.*, **52,** 75–91.

Crawford, T. M., and H. B. Bluestein, 1997: Characteristics of dryline passage during COPS-91. *Mon. Wea. Rev.*, **125,** 463–477.

Doswell, C. A., III, 1987: The distinction between large-scale and mesoscale contributions to severe convection. A case study example. *Wea. Forecasting*, **2,** 3–16.

Fujita, T. T., 1958: Structure and movement of a dry front. *Bull. Amer. Meteor. Soc.*, **39,** 574–582.

Guo, Y.-R., Y.-H. Kuo, J. Dudhia, D. Parsons, and C. Rocker, 2000: Four-dimensional variational data assimilation of heterogeneous mesoscale observations for a strong convective case. *Mon. Wea. Rev.*, **128,** 619–643.

Hane, C. E., C. L. Zeigler, and H. B. Bluestein, 1993: Investigations of the dryline and convective storms initiated along the dryline: Field experiments during COPS-91. *Bull. Amer. Meteor. Soc.*, **74,** 2133–2145.

Hogg, D. C., F. O. Guiraud, J. B. Snider, M. T. Decker, and E. R. Westwater, 1983: A steerable dual-channel microwave radiometer for measurement of water vapor and liquid in the troposphere. *J. Appl. Meteor.*, **22,** 789–806.

Holton, J. R., 1967: The diurnal boundary layer wind oscillation above sloping terrain. *Tellus*, **19,** 199–205.

Koch, S. E., and J. McCarthy, 1982: The evolution of an Oklahoma dryline. Part II: Boundary layer forcing of mesoconvective systems. *J. Atmos. Sci.*, **39,** 237–257.

——, and W. L. Clark, 1999: A nonclassical cold front observed during COPTS-91: Frontal structure and the process of severe storm initiation. *J. Atmos. Sci.*, **56,** 2862–2890.

McCarthy, J., and S. E. Koch, 1982: The evolution of an Oklahoma dryline. Part I: Meso- and subsynoptic-scale analysis. *J. Atmos. Sci.*, **39,** 225–236.

Neiman, P. J., and R. M. Wakimoto, 1999: The interaction of a Pacific

cold front with shallow air masses east of the Rocky Mountains. *Mon. Wea. Rev.,* **127,** 2102–2127.

——, M. A. Shapiro, R. M. Hardesty, B. B. Stankov, R. T. Lawrence, R. J. Zamora, and T. Hampel, 1988: The pulsed Doppler lidar: Observations of frontal structures and the planetary boundary layer. *Mon. Wea. Rev.,* **116,** 1671–1681.

NSSP Staff, 1963: Environmental and thunderstorm structures as shown by National Severe Storms Project observations in spring 1960 and 1961. *Mon. Wea. Rev.,* **91,** 271–292.

Ogura, Y., and Y. Chen, 1977: A life history of an intense mesoscale convective storm in Oklahoma. *J. Atmos. Sci.,* **34,** 1458–1476.

——, H.-M. Juang, K.-S. Zhang, and S.-T. Soon, 1982: Possible triggering mechanisms for severe storms in SESAME-AVE IV (9–10 May 1979). *Bull. Amer. Meteor. Soc.,* **63,** 503–515.

Parrish, T. R., A. R. Rodi, and R. D. Clark, 1988: A case study of the summertime Great Plains low-level jet. *Mon. Wea. Rev.*, **116,** 94–105.

Parsons, D. B., 1992: An explanation for intense frontal updrafts and narrow cold-frontal rainbands. *J. Atmos. Sci.,* **49,** 1810–1825.

——, M. A. Shapiro, R. M. Hardesty, R. J. Zamora, and J. M. Intrieri, 1991: The fine-scale structure of a west Texas dryline. *Mon. Wea. Rev.,* **119,** 1242–1258.

Post, M. J., and W. D. Neff, 1986: Doppler lidar measurements of winds in a narrow mountain valley. *Bull. Amer. Meteor. Soc.,* **67,** 274–281.

Rhea, J. O., 1966: A study of thunderstorm formation along drylines. *J. Appl. Meteor.,* **5,** 58–63.

Rotunno, R., J. B. Klemp, and M. L. Weisman, 1988: A theory for strong, long-lived squall lines. *J. Atmos. Sci.,* **45,** 463–485.

Sangster, W. E., 1987: An improved technique for computing the horizontal pressure-gradient force at the earth's surface. *Mon. Wea. Rev.,* **115,** 1358–1369.

Schaefer, J. T., 1974a: A simulative model of dryline motion. *J. Atmos. Sci.,* **31,** 956–964.

——, 1974b: The life cycle of the dryline. *J. Appl. Meteor.,* **13,** 444–449.

——, 1986: The dryline. *Mesoscale Meteorology and Forecasting,* P. S. Ray, Ed., Amer. Meteor. Soc., 549–572.

Shapiro, M. A., 1982: Mesoscale weather systems of the central United States. CIRES, 78 pp. [Available from Cooperative Institute for Research in Environmental Sciences, Boulder, CO 80309.]

——, T. Hampel, D. Rotzoll, and F. Mosher, 1985: The frontal hydraulic head: A micoscale (~1 km) triggering mechanism for mesoconvective weather systems. *Mon. Wea. Rev.,* **113,** 1166–1183.

Shaw, B. L., R. A. Pielke, and C. L. Zeigler, 1997: A three-dimensional numerical simulation of a Great Plains dryline. *Mon. Wea. Rev.,* **125,** 1489–1506.

Sun, W.-Y., and Y. Ogura, 1979: Boundary layer forcing as a possible trigger to a squall-line formation. *J. Atmos. Sci.,* **36,** 235–254.

——, and C.-C. Wu, 1992: Formation and diurnal variation at the dryline. *J. Atmos. Sci.,* **49,** 1606–1619.

Trier, S. B., D. B. Parsons, and J. H. E. Clark, 1991: Environment and evolution of a cold-frontal mesoscale convective system. *Mon. Wea. Rev.,* **119,** 2429–2455.

Wakimoto, R. M., W.-C. Lee, C.-H. Liu, and P. H. Hildebrand, 1996: ELDORA observations during VORTEX 95. *Bull. Amer. Meteor. Soc.,* **77,** 1465–1481.

Ziegler, C. L., and C. E. Hane, 1993: An observational study of the dryline. *Mon. Wea. Rev.,* **121,** 1134–1151.

——, and E. N. Rasmussen, 1998: The initiation of moist convection at the dryline: Forecasting issues from a case study perspective. *Wea. Forecasting,* **13,** 1106–1130.

——, W. J. Martin, R. A. Pielke, and R. L. Walko, 1995: A modeling study of the dryline. *J. Atmos. Sci.,* **52,** 263–285.

——, T. J. Lee, and R. A. Pielke, 1997: Convective initiation at the dryline: A modeling study. *Mon. Wea. Rev.,* **125,** 1001–1026.